Influence of internal and external factors on a controlled quadrotor flight

I. Shapovalov, V. Soloviev, V. Finaev, D. Beloglazov, J. Zargaryan, and E. Kosenko

Abstract **—**A dynamical model of quadrotor contains a number of non-linear internal and external influencing factors. Analysis of these factors influence is essential for the development of a qualitative flight control system. The impact of gyroscopic effect, centripetal acceleration and wind on the quadrotor motion are considered in this paper. Wherein, the flight is controlled by the cascade PDD^2 controller. We assessed the degree of the considered factors influence on the changing of the quadrotor state variables by modeling.

Keywords **—** Dynamics, model factors, PDD^2-controller, quadrotor.

I. Introduction

Researching of unmanned aerial vehicles (UAVs) has recently received considerable attention [1] – [4]. UAVs are used for rescue operations, reconnaissance, area protection, monitoring of industrial oblects, aerial photography, etc. The main advantage of UAVs is their compactness. So they can be used for operations in difficult terrain conditions.

Rotary-wing UAVs have significant advantages comparing with UAVs of aircraft type if one needs performing a vertical take-off and landing, motionless hovering in the air, or motion at a low velocity.

Rotary-wing UAVs with four propellers are called quadrotors. The quadrotors have increased carrying capacity, simple construction of rotors, and symmetrical structure. Rotating propellers of the quadrotor create a vertical thrust. The diagonally placed propellers rotate in opposite directions. This provides compensation of the counter-torques created by the propellers. Different modes of the quadrotor flight are the result of the variable ratio between the rotary speeds of the propellers.

From the control point of view quadrotors belong to the class of nonlinear underactuated dynamical systems. To control such systems, special approaches are used, the basic principle of which is to divide the set of state variables to the controlled and stabilized [5], [6].

Since the quadrotor is an autonomous vehicle, the approaches developed to control the motion of autonomous mobile robots can be applied to control it. Conventional controllers based on the PID law [7], [8], the adaptive control [9] - [11], the robust control [12] - [14], as well as intelligent controllers based on fuzzy logic [15], and artificial neural networks [16] are often used for the vehicle control. Nowadays, the hybrid approach is considered as the most promising in the terms of control in uncertain environments and/or with uncertain vehicle parameters [17], [18]. In the hybrid approach conventional and intelligent controllers are combined. The conventional part of controller operates in the most of UAV flight modes. The intelligent part comes into operation in cases where the quality of control becomes unsatisfactory under the influence of uncertainties and nonlinearities.

The development of a hybrid control system requires a qualitative description and model of the control object. It is necessary to identify the switching conditions between the conventional and intelligent parts of the quadrotor flight controller. Analysis of the model allows understanding the dynamical processes that are typical for the quadrotor flight, and synthesis of the high-quality hybrid motion controllers.

We need assessment of external disturbances, gyroscopic effect and inertial forces affecting the quadrotor for analysis of operation modes. The character of disturbances depends on the environment and changes uninterruptedly. But the influence of inertial forces and gyroscopic effect is determined by the parameters of quadrotor construction and by the flight mode.

In the works on the UAV dynamics known to us, or no attention is paid to analysis of the contribution of individual model components in the flight dynamics [7], [19] - [23], or paid insufficiently [1, 3, 24]. Therefore, in this paper we have tried to represent our research results concerning the effect of centripetal acceleration, gyroscopic effect and wind disturbance on the dynamics of quadrotor flight controlled by the cascade PDD^2 controller. The choice of such type of control was stipulated by the need to analyze the limits of the

This work was supported by the Russian Scientific Foundation Grant 14-19-01533 and made at the Southern Federal University, Russia.

I. Shapovalov is with the Southern Federal University, Rostov-on-Don, Russia (+7(8634)37-16-89; e-mail: shapovalovio@gmail.com).

V. Soloviev is with the Southern Federal University, Rostov-on-Don, Russia (+7(8634)37-16-89; e-mail: soloviev-tti@mail.ru).

V. Finaev, is with the Southern Federal University, Rostov-on-Don, Russia (+7(8634)37-17-73; e-mail: finaev_val_iv@tgn.sfedu.ru).

D. Beloglazov is with the Southern Federal University, Rostov-on-Don, Russia (e-mail: d.beloglazov@gmail.com).

J. Zargaryan is with the Southern Federal University, Rostov-on-Don, Russia (+7(8634)37-16-89; e-mail: jury.zargaryan@gmail.com).

E. Kosenko is with the Southern Federal University. Rostov-on-Don. Russia (+7(8634)37-16-89: fax: +7(8634) 37-16-89: e-mail: kosenko@tti.sfedu.ru).

convenient PD controller applicability to the complex dynamical modes as a part of hybrid control system.

The paper [25] contains analysis of gyroscopic effect, centripetal acceleration and Coriolis force influence on the flight of helicopter. There is still no such high-quality work dedicated to the quadrotor dynamics. Therefore, the results of [25] – [27] are the base for the analysis of the quadrotor behavior with a consideration of similarities and differences of helicopter and quadrotor models.

II. Mathematical Model

We described the quadrotor flight through conceptions of inertial and body-fixed coordinate frames [28]. The inertial frame $0_o X_g Y_g Z_g$ is connected with the earth. The body fixed frame $0XYZ$ is rigidly connected with the quadrotor. Fig. 1 shows the quadrotor with the relevant coordinate frames.

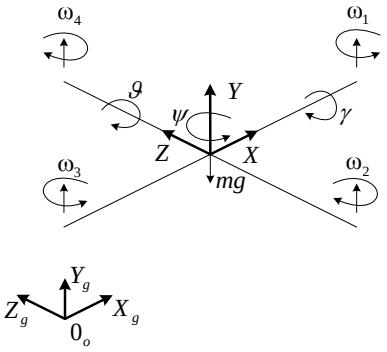

Fig. 1 Simplified representation of quadrotor

We developed equations of motion with respect to $0XYZ$ frame for the following reasons: the matrix of inertia moments is invariant; equations of motion are simple due to the quadrotor model symmetry; on-board measures can be easily used; lift force doesn't change its orientation.

Lift forces of the rotors change orientation and position of $0XYZ$ frame with respect to $0_o X_g Y_g Z_g$ frame. The rotation rate of propellers determines the value of lift forces. The quadrotor moves strictly vertically when the lift forces of propellers are equal. The quadrotor orientation changes when the torques are not compensated. Torques appear because of unbalanced rotation rates of the propellers. If the angles of roll and pitch are nonzero, the lift forces have nonzero components on the plane $0_o X_g Z_g$. These components provoke horizontal motion of the quadrotor.

The position of $0XYZ$ frame with respect to $0_o X_g Y_g Z_g$ frame is described by the coordinate vector $\xi=[x, y, z]$, and orientation is described by the vector $\eta=[\gamma, \vartheta, \psi]$ of roll, pitch and yaw angles. The vector $V=[V_X, V_Y, V_Z]$ describes the linear velocity of quadrotor in body-fixed frame. The vector $\Omega=[\Omega_X, \Omega_Y, \Omega_Z]$ describes the angular velocity of quadrotor in body-fixed frame. Because of two coordinate frames, we use operators for transformation of linear and angular variables. We describe the relation between linear and angular velocities in body-fixed and inertial frames by formulas [6]:

$$\dot{\xi}=R_t V,\ \Omega=R_r\dot{\eta}, \tag{1}$$

where R_t, R_r are the matrixes of linear and angular variables transformation.

Transformation matrix for linear variables from $0XYZ$ frame to $0_o X_g Y_g Z_g$ frame is

$$R_t=\begin{bmatrix} c\psi c\vartheta & s\psi s\gamma - c\psi s\vartheta c\gamma & s\psi c\gamma + c\psi s\vartheta s\gamma \\ s\vartheta & c\vartheta c\gamma & -c\vartheta s\gamma \\ -s\psi c\vartheta & c\psi s\gamma + s\psi s\vartheta c\gamma & c\psi c\gamma - s\psi s\vartheta s\gamma \end{bmatrix}, \tag{2}$$

where we denote $c\leftrightarrow\cos$, $s\leftrightarrow\sin$.

Transformation matrix for angular variables from $0XYZ$ frame to $0_o X_g Y_g Z_g$ frame is

$$R_r=\begin{bmatrix} 1 & \cos\gamma\tan\vartheta & \sin\gamma\tan\vartheta \\ 0 & \cos\gamma/\cos\vartheta & -\sin\gamma/\cos\vartheta \\ 0 & \sin\gamma & \cos\gamma \end{bmatrix}. \tag{3}$$

Derivation of equations describing dynamics of quadrotors is carried out with the use of Euler-Langrage formalism [3], [7], [29], or on the basis of Newton laws [19], [24], [30]. Let's consider equations on the basis of Newton laws of mechanics, because this approach is more intuitive. The matrix equitation of quadrotor dynamics in body-fixed frame is

$$\begin{bmatrix} mE & 0_{3\times3} \\ 0_{3\times3} & I \end{bmatrix}\cdot\begin{bmatrix} \dot{V} \\ \dot{\omega} \end{bmatrix}+\begin{bmatrix} \Omega\times(mV) \\ \Omega\times(I\Omega) \end{bmatrix}=\begin{bmatrix} F \\ M \end{bmatrix}, \tag{4}$$

where m is the mass of quadrotor; E is the identity matrix of size 3×3; I is the diagonal matrix of quadrotor inertia moments; V is the linear velocity of quadrotor; Ω is the angular velocity of quadrotor; F is the force vector affecting quadrotor; M is the vector of torques.

The second term in the left part of equation (4) determines the influence of inertial forces and has form

$$\begin{bmatrix} \Omega\times(mV) \\ \Omega\times(I\Omega) \end{bmatrix}=\begin{bmatrix} \Omega_X & \Omega_Y & \Omega_Z \end{bmatrix}\begin{bmatrix} 0 & -mV_Z & mV_Y \\ mV_Z & 0 & -mV_X \\ -mV_Y & mV_X & 0 \\ 0 & -I_{zz}\Omega_Z & I_{yy}\Omega_Y \\ I_{zz}\Omega_Z & 0 & -I_{xx}\Omega_X \\ -I_{yy}\Omega_Y & I_{xx}\Omega_X & 0 \end{bmatrix}, \tag{5}$$

where $I=\begin{bmatrix} I_{xx} & 0 & 0 \\ 0 & I_{yy} & 0 \\ 0 & 0 & I_{zz} \end{bmatrix}$.

There are five components characterizing forces and torques effecting on the quadrotor in the right part of equation (4). The first component is the vector of gravity force:

$$F_G=R_t^{-1}F_{G_o}=R_t^{-1}\begin{bmatrix} 0 \\ -mg \\ 0 \end{bmatrix}=\begin{bmatrix} -mgs\vartheta \\ -mgc\vartheta c\gamma \\ mgc\vartheta s\gamma \end{bmatrix}, \tag{6}$$

where F_{G_o} is the gravity vector in inertial frame; F_G is the gravity vector in body-fixed frame; g is the free fall acceleration.

The second component is gyroscopic effect. Gyroscopic effect arises when the shafts of motors change their orientation. The second component influences only the change of angular components of dynamics and is described by expression

$$M'_{gyr} = -\sum_{k=1}^{4} J_r \left(\Omega \times \begin{bmatrix} 0 \\ 1 \\ 0 \end{bmatrix} \right) (-1)^k \omega_k =$$

$$= J_r \begin{bmatrix} -\Omega_Z \\ 0 \\ \Omega_X \end{bmatrix} \varpi = J_r \begin{bmatrix} \Omega_Z & -\Omega_Z & \Omega_Z & -\Omega_Z \\ 0 & 0 & 0 & 0 \\ -\Omega_X & \Omega_X & -\Omega_X & \Omega_X \end{bmatrix} \varpi , \quad (7)$$

where J_r is the inertia moment of motor with propeller; $\varpi = \begin{bmatrix} \omega_1 & \omega_2 & \omega_3 & \omega_4 \end{bmatrix}^T$ is the vector of rates of propellers.

The third component is lift force and torques of rotors. These force and torques are proportional to the squared rotation rates of propellers and can be described by expression

$$U = \begin{bmatrix} U_1 \\ U_2 \\ U_3 \\ U_4 \end{bmatrix} = \begin{bmatrix} b(\omega_1^2 + \omega_2^2 + \omega_3^2 + \omega_4^2) \\ bl(\omega_4^2 - \omega_2^2) \\ bl(\omega_3^2 - \omega_1^2) \\ d(\omega_2^2 + \omega_4^2 - \omega_1^2 - \omega_3^2) \end{bmatrix}, \quad (8)$$

where l is the distance between the center of quadrotor symmetry and motor shafts; b, d are the proportional coefficients. Equitation (8) doesn't take into account the component of angular acceleration of motor shafts.

The forth component is aerodynamic forces and moments. The air drag force is determined by expression

$$F_{AG} = -A \cdot \begin{bmatrix} |V_X| \cdot V_X \\ |V_Y| \cdot V_Y \\ |V_Z| \cdot V_Z \end{bmatrix} = \begin{bmatrix} -A_X \cdot |V_X| \cdot V_X \\ -A_Y \cdot |V_Y| \cdot V_Y \\ -A_Z \cdot |V_Z| \cdot V_Z \end{bmatrix}, \quad (9)$$

where A is the diagonal matrix of drag force coefficients.

In [31] - [34] the fifth component is described. It is the impact of meteorological factors. The main meteorological factors include: a change in temperature, pressure, air density and movement of air masses (wind) [34]. The wind has the greatest influence on the dynamics of flight. Effect of changes in temperature, pressure and air density is not so much on the operational altitudes of the quadrotor.

The force with which the wind acts on the quadrotor is given by

$$F_w = R_t^{-1} S_e A \left(V_{wy}\right)^2 = \begin{bmatrix} S_{ex} A \left(V_{wy}\right)^2 \cos\psi_w \sin\vartheta \\ 0 \\ -S_{ez} A \left(V_{wy}\right)^2 \sin\psi_w \cos\vartheta \sin\gamma \end{bmatrix}, \quad (10)$$

where S_e is the influence effective area; A=(1/16)·9,81=0,61 is the rate of wind velocity conversion to pressure [34]; V_{wy} is the wind velocity at altitude y, ψ_w is the direction of wind.

Let's represent a quadrotor as a cylinder component for the simplicity sake. The expression determining the quadrotor surface area will be equal to the sum of the area Sb of the lateral surface and the area So of bases

$$S_k = S_b + S_0 = \alpha 2\pi r h + \beta 2\pi r^2 , \quad (11)$$

where h is the cylinder height, r is the cylinder radius, α, β are the fill factors of the cylinder area (depending on quadrotor design).

The first term in (11) determines the area of the cylinder lateral surface; the second term determines the area of the cylinder bases. We assume that the wind has a uniform impact on the construction of quadrotor as it shown in Fig. 2.

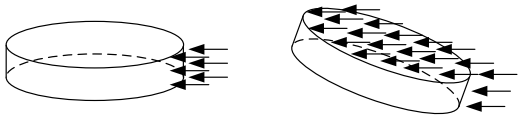

Fig. 2 Wind effect on a quadrotor construction

Let wind effects half a quadrotor area. Taking into account (9) we will get the expression for the effective area:

$$S_{ex} = \beta\pi r^2 s\gamma + \alpha\pi r h c\gamma, \; S_{ez} = \beta\pi r^2 s\vartheta + \alpha\pi r h c\vartheta . \quad (12)$$

Full equations of the quadrotor dynamics in the body-fixed frame have form

$$\begin{cases} \dot{V}_X = (V_Y\Omega_Z - V_Z\Omega_Y) + g s_\vartheta - A_X \cdot |V_X| \cdot V_X + \\ + S_{ex} A \left(V_{wy}\right)^2 c\psi_w s\vartheta, \\ \dot{V}_Y = (V_Z\Omega_X - V_X\Omega_Z) - g c_\vartheta c_\gamma + \dfrac{U_1}{m} - A_Y \cdot |V_Y| \cdot V_Y , \\ \dot{V}_Z = (V_X\Omega_Y - V_Y\Omega_X) - g c_\vartheta s_\gamma - A_Z \cdot |V_Z| \cdot V_Z - \\ - S_{ez} A \left(V_{wy}\right)^2 s\psi_w c\vartheta s\gamma, \\ \dot{\Omega}_X = \dfrac{I_{yy} - I_{zz}}{I_{xx}} \Omega_Y\Omega_Z - \dfrac{J_{\check{N}Đ}}{I_{xx}} \Omega_Z \varpi + \dfrac{U_2}{I_{xx}}, \\ \dot{\Omega}_Y = \dfrac{I_{zz} - I_{xx}}{I_{yy}} \Omega_X\Omega_Z + \dfrac{U_3}{I_{yy}}, \\ \dot{\Omega}_Z = \dfrac{I_{xx} - I_{yy}}{I_{zz}} \Omega_X\Omega_Y + \dfrac{J_{\check{N}Đ}}{I_{yy}} \Omega_X \varpi + \dfrac{U_4}{I_{zz}}. \end{cases} \quad (13)$$

The first terms on the right side of equations (13) describe the effect of Coriolis and centripetal forces on the motion of quadrotor [24, 35]. The influence of gyroscopic effect on the quadrotor dynamics becomes apparent when the orientation of motor shafts changes [36]. One can observe the influence of centripetal force when the angular velocity of quadrotor has more than one non-zero component relative to the axes of body-fixed frame. It can be called either a centripetal acceleration effect [24, 37] or the gyroscopic effect of the rigid body rotation [3].

The dynamics of brushless DC motors most commonly used in quadrotors is described by equations

$$U_i = R i_i + L \frac{di_i}{dt} + k_e \omega_i , \quad (14)$$

$$\dot{\omega}_i = k_M i_i - d\omega_i^2 , \quad (15)$$

where U_i, i_i, ω_i are the voltage, the current and the shaft rotation rate of the i-th motor; R and L are the resistance and inductance of the stator winding; k_e and k_M are the constructive elements of motor; d is the air drag coefficient.

III. Gyroscopic effect influence

Gyroscopic effect is observed in systems with noncollinearity of a rotation axis and the resultant vector of applied torques [36].

Fig. 3 shows the disk representing the quadrotor structure, the inertial frame $0_oX_gY_gZ_g$, and the body-fixed frame $0XYZ$. The frame $0XYZ$ is rigidly connected with the disk in such a way that frame origin matches with the disk center, and the disk plane lies on the plane $0XZ$. The disk rotates around $0Y$ axis with a velocity ω_y. The torque determined by the cross product $[\omega_x, \omega_y]$ arises as a result of two orthogonal rotation vectors interaction.

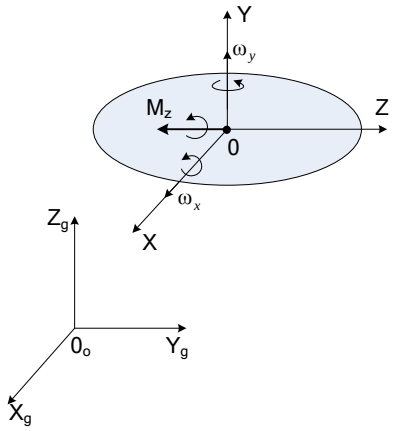

Fig. 3 Gyroscopic effect influence

We suppose that in initial state the quadrotor is hovering above the earth. Let's consider the influence of gyroscopic effect on the turn of quadrotor around every axis of the body-fixed frame. We introduce four additional coordinate frames $0X_iY_iZ_i$, axes of which are directed as the corresponding axes of $0XYZ$ frame and origins are located in the points of intersection of axes $0X$ and $0Z$ with the shafts of motors.

To rotate the quadrotor clockwise around $0Y$ without changing of a position, it's necessary to increase ω_2 and ω_4, and decrease ω_1 and ω_3 (see fig. 1). The motor shafts and axis $0Y$ are collinear, and their cross product is equal to zero, so gyroscopic effect doesn't occur.

For the quadrotor clockwise rotation around $0X$, it's necessary to increase ω_4 in comparison with ω_2. The quadrotor rotation around $0X$ has a velocity ω_x. The angular velocity ω_x is equal for all four rotor frames, although the second and the forth rotors perform larger linear movement in inertial frame comparing with the first and the third rotors.

When the quadrotor rotates around $0X$ axis, four torques appear. These torques tend to turn the motors with propellers around axes $0Y_i$, $i=\overline{1,4}$.

The value of resulting torque caused by gyroscopic effect is determined by expression

$$M_z = -M_{z1} + M_{z2} - M_{z3} + M_{z4} = \omega_x \cdot (-\omega_1 + \omega_2 - \omega_3 + \omega_4). \quad (16)$$

This expression allows making conclusion that gyroscopic effects of motors will be compensated and will not influence the quadrotor dynamics when the condition $|\omega_1+\omega_3|=|\omega_2+\omega_4|$ is satisfied. If $|\omega_1+\omega_3|>|\omega_2+\omega_4|$, the torque rotating the quadrotor clockwise around $0Z$ will appear. If $|\omega_1+\omega_3|<|\omega_2+\omega_4|$, the torque will rotate the quadrotor counter-clockwise.

Analysis of the gyroscopic effect influence in the case of quadrotor rotation around $0Z$ axis with a velocity ω_z can be provided in a similar way.

IV. Centripetal acceleration influence

In this section we suppose the quadrotor hovering above the earth and rotating clockwise around $0Y$ axis in the initial state ($|\omega_2+\omega_4|>|\omega_1+\omega_3|>0$). We considered the influence of gyroscopic effect when the quadrotor rotates around axes $0X$ and $0Y$ of the body-fixed frame.

Let's imagine the quadrotor rotates clockwise around $0Y$ axis and simultaneously rotates clockwise around $0X$ axis. As a result the torque M_{zk} determined by the cross production $[\omega_x, \omega_y]$ appears. This torque turns the quadrotor counter-clockwise around the axis $0Z$.

The torque M_{xk} appears when the quadrotor rotates clockwise around $0Y$ and simultaneously clockwise around $0Z$. This torque determined by the cross product $[\omega_z, \omega_y]$ tends to rotate the quadrotor around $0X$ axis.

V. Influence of wind

Analysis of wind effect allows separation the constant (systematic) component and the variable (turbulent) component. The constant component specifies a constant wind velocity value. The variable component specifies gusts. Estimation of main meteorological conditions influence is often made with using statistical models of meteorological conditions deviation from their climatic values [38]. The wind velocity will be considered as a vector random value in this paper. The wind velocity is defined in the point $r=(x,y,z)$ by the formula

$$V_w(r)=V_s(r)+V_v(r), \quad (17)$$

where $V_w(r)$ is the full wind velocity, $V_c \in \mathrm{R}^3$ is the systematic component, $V_v \in \mathrm{R}^3$ is the variable component.

The proposed model of the gust wind is specified with the following expression

$$|V_w| = \begin{cases} V_{w0}, & t \le t_0, \\ V_{w0} + \dfrac{|V_m - V_{w0}|}{2}\left(1 - \cos\left(\dfrac{\pi(t-t_0)}{d_{d'}-t_0}\right)\right), & \\ t_0 < t \le d_{d'}, V_m \ge V_{w0}, & \\ V_{w0} + \dfrac{|V_m - V_{w0}|}{2}\left(\cos\left(\dfrac{\pi(t-t_0)}{d_{d'}-t_0}\right) - 1\right), & \\ t_0 < t \le d_{d'}, V_m < V_{w0}, & \\ V_m, & t \le t_{m.} \end{cases} \quad (18)$$

where V_{w0} is the wind velocity before the "step", V_m is the maximum admissible velocity, t_0 is the start moment of gust, t_m is the time of modeling, d_n is the interval of wind changing.

The simulation results at t_0=[0; 9; 16; 19] (s), V_m=[1; 4.5; 0; 1] (m/s), d_n=[7; 5; 2; 5] (s), t_m=25 s, V_{w0}=0.5 m/s are shown in Fig. 4.

The simulation results reveal that model (18) allows simulation the increase and decrease of wind velocity taking into account the velocity of wind before "step". Using this model the systematic component V_s of wind velocity can be simulated.

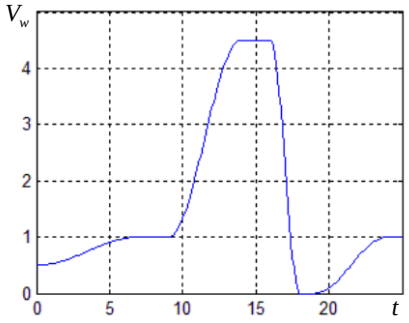

Fig. 4. Changing of wind velocity

To simulate the wind velocity changes depending on altitude we will use the following formula

$$V_{wy} = V_{0y}\left(\frac{y}{y_0}\right)^p, \tag{19}$$

where V_{0y} is the specified (measured) wind velocity at altitude y_0, p is the index of energetic wind profile.

The diagram of wind velocity depending on altitude is shown in Fig. 5. The model (19) has shown satisfactory results at difference y-y_0 less than 50 meters (V_{w0}=3 m/s, y_0=1 m, p=0.1).

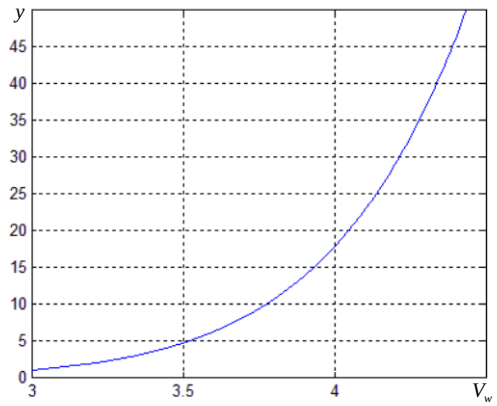

Fig. 5 Diagram of wind velocity depending on altitude

VI. Control System

Since some components of equations (13) effect the flight dynamics, make model nonlinear, and complicate the analysis of quadrotor behavior, the control system design is rather complex. Therefore, we made the tuning of control system on the simplified model described by equations

$$\begin{cases} \dot{V}_X = gs\vartheta, \\ \dot{V}_Y = gc\vartheta c\gamma + \dfrac{U_1}{m}, \\ \dot{V}_Z = gc\vartheta s\gamma, \\ \dot{\Omega}_X = \dfrac{U_2}{I_{xx}}, \\ \dot{\Omega}_Y = \dfrac{U_3}{I_{yy}}, \\ \dot{\Omega}_Z = \dfrac{U_4}{I_{zz}}. \end{cases} \tag{20}$$

When the quadrotor takes-off from earth to a desired altitude, the orientation angles do not change, so the system is linear. Simple PID controllers are appropriate for such systems control. We decided, it is best to apply the PD controller to increase the quadrotor stability, because the transfer function between the forces acting in vertical plane and y coordinate is integrator of the second order.

When quadrotor flights in complex dynamic modes, nonlinearities of the system begin to play an increasingly important role. Furthermore, when we try to control multiple channels with double integration, the problem of stability ensuring becomes very difficult. So we decided to control not the coordinates, but the velocity with PDD^2 controller. The structure of controller tuned through equations (20) is shown in Fig. 6.

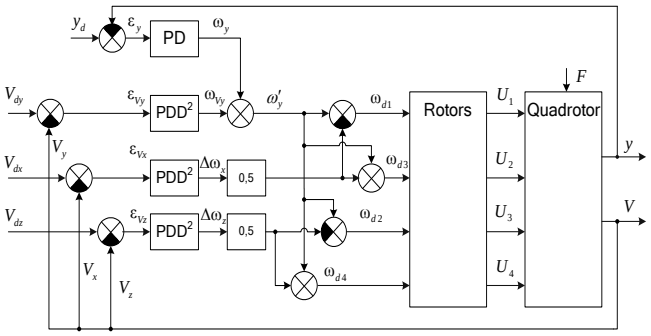

Fig. 6 Block-diagram of cascade PDD^2 control system

We used the following notations in Fig. 6: y_d is the desired altitude (sustained in the hovering mode); y is the altitude of quadrotor; $\varepsilon = \begin{bmatrix} \varepsilon_{Vy} & \varepsilon_{Vx} & \varepsilon_{Vz} \end{bmatrix}$ is the vector of velocity deviation from desire[t, s] ue; ω_y is the output of altitude controller; ω_{Vy}, $\Delta\omega_x$, $\Delta\omega_z$ are outputs of velocity controllers; ω_{di} is the desired value of the i-th motor rotational speed; $U_{1\text{-}4}$ are the force and torques from equation (8); F is the vector of external disturbances. The block Rotors includes the embedded PD-controllers of rotational speed.

VII. Simulation

For quantitative assessment of the gyroscopic effect, centripetal acceleration, and friction force influence on the quadrotor flight modes characterized by angular coordinates

changing, we developed simulation model in Simulink on the basis of equations (13). In the research we used the following values of model parameters: $J_r = 73.9 \cdot 10^{-6}$ kg·m^2; $m = 1$ kg; $I_{XX} = I_{YY} = 0.081$ kg·m^2; $I_{ZZ} = 0.142$ kg·m^2; $l = 0.24$ m; $b = 53.81 \cdot 10^{-6}$ N·s^2/rad^2; $d = 1.1 \cdot 10^{-6}$ N·m·s^2/rad^2; $A_{X'} = A_{Y'} = A_{Z'} = 1$ kg/m, $V_m = 5$ m/s. Initially the quadrotor was in a motionless state on the earth and had coordinates ξ=[0, 0, 0], rotational speeds of propellers were ω_i=0 rad/s, $i = \overline{1,4}$. The parameters of motors were taken from [24].

The simulation was performed in the following scenario: the quadrotor took-off to hovering at the altitude y = 1 m, then in t=5 s the quadrotor moved in accordance with a desired velocity vector $\dot{\xi}_d = [\sin(t), 0.5, \sin(t + \pi/2)]$. Table I shows the values of integral quadratic differences: a) between the rotary rates of the propellers in the simplified model (20) and the rotary rates in the model (13) without friction and wind (e_1); b) between the rotary rates of the propellers in the simplified model (20) and the rotary rates in the model (13), taking into account all factors (e_2).

Table I

Difference between rotary speeds of propellers

	Propeller 1	Propeller 2	Propeller 3	Propeller 4
$e_1 \cdot 10^{-3}$	9,32	20,87	9,53	20,58
$e_2 \cdot 10^{-3}$	621,81	620,95	621,95	621,44

Fig. 7 and Fig. 8 show the results of simulation for three quadrotor dynamic models: the model (20), the model (13) without the friction force and wind, and the full model (13).

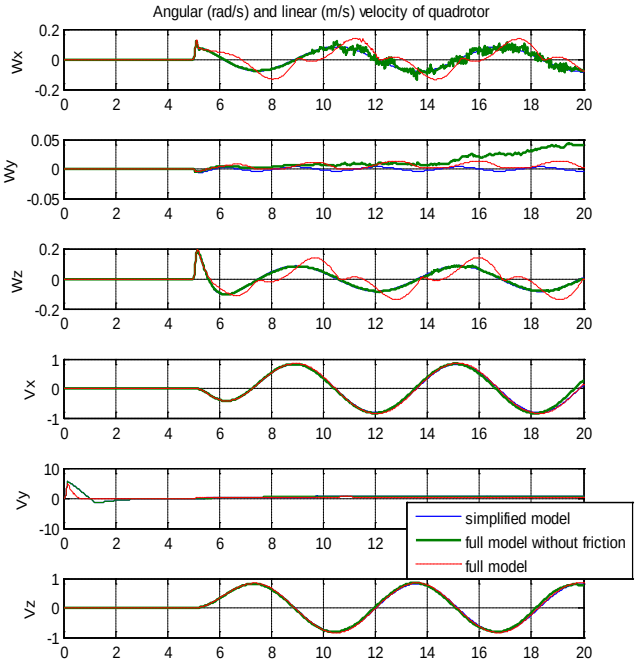

Fig. 7 Components of quadrotor linear and angular velocity in inertial frame

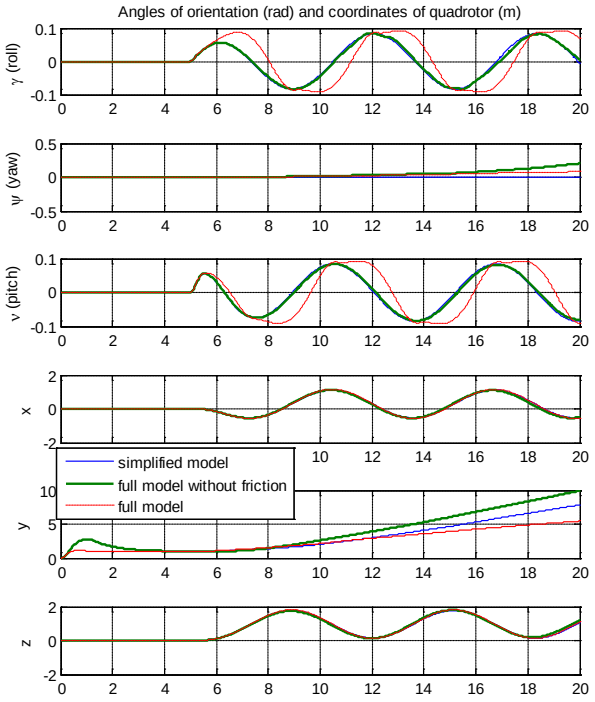

Fig. 8 Quadrotor linear and angular coordinates in inertial frame

The curves in Fig. 7 representing behavior of the full model without friction have some noise caused by the discrete PDD^2 control. Such noise is one of main disadvantages of the PDD^2 control. Also Fig. 7 shows that aerodynamic friction force makes the noise of PDD^2 control damping.

Character of difference between the curves in Fig. 7 and Fig. 8 proves very important role of the aerodynamic effects (friction force and wind in our case) in the flight control.

VIII. Conclusions

To analyze the behavior of quadrotor in space, we need to consider all set of factors affecting it. For this purpose we derived the model of quadrotor dynamics in the form of differential equations. The model takes into account various types of external and internal forces and torques including gravity force, gyroscopic effect, forces and moments of rotors, centripetal acceleration, Coriolis force, and aerodynamic friction force.

We have analyzed the influence of gyroscopic effect, centripetal acceleration, and wind on the quadrotor motion in details. Research was carried out in the conditions of rotor shaft orientation changing and when the rotation speed of quadrotor has more than one nonzero component in body-fixed frame.

We designed the cascade control system based on PD (PDD^2) control law to estimate the influence of researched effects on the controlled flight dynamics of quadrotor. Tuning of the controllers was made on the simplified model.

The simulation results showed that centripetal acceleration, gyroscopic effect and Coriolis force have a significant influence on the change of angular variables. Friction force and wind have even more noticeable impact on the angular variables. What concerns linear variables, only altitude and rate of rise appreciably depend on the model completeness.

We think that results of performed research can be used in the tasks of quadrotor flight control. Our research allows understanding the peculiarities and character of disturbances in the control model. Taking into account these disturbances gives the opportunity to effectively solve flight control tasks.

REFERENCES

[1] P. McKerrow, "Modelling the Draganflyer four-rotor helicopter," in Proc. IEEE International Conference on Robotics and Automation, vol. 4, pp. 3596-3601, 2004.

[2] D. Mellinger, N. Michael, V. Kumar, "Trajectory generation and control for precise aggressive maneuvers with quadrotors," International Journal of Robotics Research, vol. 31(5), pp. 664-674, 2012.

[3] S. Bouabdallah, "Design and control of quadrotors with application to autonomous flying" // Ph.D. dissertation, Laboratoire de systèmes autonomies, École polytechnique fédérale de Lausanne EPFL, Lausanne, 2006.

[4] K. P. Valavanis, M. Kontitsis, " A historical perspective on unmanned aerial vehicles," in *Advances in Unmanned Aerial Vehicles: State of the Art and the Road to Autonomy*, K. P. Valavanis, Ed. Dordrecht: Springer, 2007, pp. 15-48.

[5] R. Olfati-Saber, "Nonlinear control of underactuated mechanical systems with application to robotics and aerospace vehicles," Ph.D. thesis, Department of Electrical Engineering and Computer Science, Massachusetts Institute of Technology, Cambridge, MA, 2001.

[6] T. Madani, A. Benallegue, "Backstepping control for a quadrotor helicopter," in Proc. IEEE/RSJ International Conference on Intelligent Robots and Systems, pp. 3255–3260, 2006.

[7] P. Castillo, A. Dzul, R. Lozano, "Real-time stabilization and tracking of a four-rotor mini rotorcraft," IEEE Transactions on Control Systems Technology, vol. 12, no. 4, pp. 510–516, 2004.

[8] A.Y. Elruby, M.M. El-Khatib, N.H. El-Amary, A.I. Hashad, "Dynamic modeling and control of quadrotor vehicle," in Proc. Fifteenth International Conference on Applied Mechanics and Mechanical Engineering (AMME-15), 2012.

[9] V. Kh. Pshikhopov, V. A. Krukhmalev, M. Yu. Medvedev, R. V. Fedorenko, S. A. Kopylov, A. Yu. Budko, V. M. Chufistov, "Adaptive control system design for robotic aircrafts," in Proc. 2013 IEEE Latin American Robotics Symposium, pp. 67-70.

[10] R. Mahony , T. Hamel, "Adaptive compensation of aerodynamic effects during takeoff and landing manoeuvres for a scale model autonomous helicopter," European Journal of Control, vol. 1, 2001, pp. 1-15.

[11] X. Gong, Z.-C. Hou, C.-J. Zhao, Y. Bai, Y.-T. Tian, "Adaptive backstepping mode trajectory tracking control for a quad-rotor," International Journal of Automation and Computing, vol. 9, no. 5, 2012, pp. 555-560.

[12] V. Kh. Pshikhopov, M. Yu. Medvedev, "Robust control of nonlinear dynamic systems," in Proc. 2010 IEEE ANDESCON Conference, pp. 1-7.

[13] V. Kh. Pshikhopov, M. Yu. Medvedev, "Block design of robust control systems by direct Lyapunov method," IFAC Proceedings Volumes (IFAC-PapersOnline), pp. 10875-10880, 2011.

[14] F. F. M. El-Sousy, "Robust hybrid control using recurrent wavelet-neural-network sliding-mode controller for two-axis motion control system," in Proc. The 2013 International Conference on Systems, Control, Signal Processing and Informatics, Rhodes Island, 2013, pp. 268-278.

[15] M. Faisal, K. Al-Mitib, R. Hedjar, H. Mathkour, M. Alsulaiman, E. Mattar, "Multi modules fuzzy logic for mobile robots navigation and obstacle avoidance in unknown indoor dynamic environment," in Proc. The 2013 International Conference on Systems, Control and Informatics, Venice, 2013, pp. 371-379.

[16] A. Serrat, M. Benyettou, "ATNN and SVM for autonomous mobile robot," in Proc. The 2013 International Conference on Systems, Control and Informatics, Venice, 2013, pp. 316-320.

[17] V. Kh. Pshikhopov, A. S. Ali, "Hybrid control of a mobile robot in dynamic environments," in Proc. 2011 IEEE International Conference on Mechatronics, pp. 540-545.

[18] V. V. Ignatyev, V. I. Finaev, "The use of hybrid regulator in design of control systems," World Applied Sciences Journal, vol. 23, no. 10, 2003, pp. 1291 – 1297.

[19] H. Bolandi, M. Rezaei, R. Mohsenipour, H. Nemati, S.M. Smailzadeh, "Attitude control of a quadrotor with optimized PID controller," Intelligent Control and Automation, vol. 4, pp. 335-342, 2013.

[20] V. Kh. Pshikhopov, M. Yu. Medvedev, A. R. Gaiduk, B. V. Gurenko, "Control system design for autonomous underwater vehicle," in Proc. 2013 IEEE Latin American Robotics Symposium, pp. 77-82.

[21] P. Pounds, R. Mahony, P. Corke, "Modelling and control of a quad-rotor robot," in Proc. Australasian Conference on Robotics and Automation, 2006.

[22] V. K. Pshikhopov, M. Yu. Medvedev, B. V. Gurenko, "Homing and docking autopilot design for autonomous underwater vehicle," Applied Mechanics and Materials, vol. 490-491, pp. 700-707, 2014.

[23] V. Pshikhopov, V. Krukhmalev, M. Medvedev, R. Neydorf, "Estimation of energy potential for control of feeder of novel cruise/feeder MAAT," SAE Technical Paper 2012-01-099, 2012.

[24] T. Bresciani, "Modelling, identification and control of a quadrotor helicopter," master's thesis, Department of automatic control, Lund University, Lund, 2008.

[25] G.D. Padfield, *Helicopter flight dynamics: the theory and application of flying qualities and simulation modelling*. 2nd ed., Washington, DC: Blackwell Publishing, 2007, ch. 3.

[26] V. Pshikhopov, M. Medvedev, V. Kostjukov, R. Fedorenko, et al., "Airship autopilot design," SAE Technical Paper 2011-01-2736, 2011.

[27] V. Pshikhopov, M. Medvedev, R. Neydorf, V. Krukhmalev, et al., "Impact of the feeder aerodynamics characteristics on the power of control actions in steady and transient regimes," SAE Technical Paper 2012-01-2112, 2012.

[28] V. Pshikhopov, N. Sergeev, M. Medvedev, A. Kulchenko, "The design of helicopter autopilot," SAE Technical Paper 2012-01-2098, 2012.

[29] G.V. Raffo, M.G. Ortega, F.R. Rubio, "Nonlinear H∞ controller for the quad-rotor helicopter with input coupling," in Proc. The 18th IFAC World Congress, pp. 13834-13839, 2011.

[30] A.A. Mian, M.I. Ahmad, D. Wang, "Backstepping based PID control strategy for an underactuated aerial robot," in Proc. The 17th IFAC World Congress, pp. 15636-15641, 2008.

[31] M.V. Cook, *Flight dynamics principles*. 2nd ed., Oxford, UK: Butterworth-Heinemann, 2007, pp. 72-73.

[32] R. Neydorf, V. Krukhmalev, N. Kudinov, V. Pshikhopov, "Methods of statistical processing of meteorological data for the tasks of trajectory planning of MAAT feeders," SAE Technical Paper 2013-01-2266, 2013.

[33] E. P. Sholny, L. A. Maiboroda, *Atmosphere and control of aerial vehicles motion*, V. M. Ponomarev, Ed., Saint-Peterburg: Hydrometeoizdat, 1973, ch. 2-3 [Школьный Е.П., Майборода Л.А. Атмосфера и управление движением летательных аппаратов. Под. Ред. проф. В.М. Пономарева. Л.: Гидрометеоиздат, 1973].

[34] V. A. Podobed, "Mathematical modeling of wind effects on dockside cranes," News of MSTU, vol. 9, no. 2, 2006, pp. 318-331 [Подобед В.А. Математическое моделирование ветровых нагрузок на портовые портальные краны // Вестник МГТУ, том 9, №2, 2006, с. 318-331].

[35] B. Etkin, *Dynamics of Atmospheric Flight*. New York: John Wiley & Sons, 1972, ch. 5.

[36] H.D. Young, R.A. Freedman, A.L. Ford, *Sears and Zemansky's university physics: with modern physics*. 13th ed., San Francisco, CA: Addison-Wesley, 2012, pp. 328-330.

[37] A.R.S. Bramwell, G. Done, D. Balmford, *Bramwell's Helicopter Dynamics*, 2nd ed., Oxford, UK: Butterworth-Heinemann, 2001, ch. 1.

[38] V. Pshikhopov, M. Medvedev, A. Gaiduk, et al. "The position-trajectory control system for robotic aerial platform. Part 1. Mathematical model," Mechatronics, automation, control, vol. 6, 2013, pp. 14-21.